Simulation and Analysis of HEMP Coupling Effect on a Wire Inside an Apertured Cylindrical Shielding Cavity

Shu-Ting Song, Hong Jiang, Yu-Lan Huang

College of Communication Engineering
Jilin University, Changchun, Jilin Province 130012, China
Email: shadoushi@163.com, jiangh@jlu.edu.cn, ylhuang@jlu.edu.cn

Abstract ─ High altitude nuclear electromagnetic pulse (HEMP) can damage electronic equipments of radar and communication systems. Back door coupling is one of the main ways of HEMP attacks on the electronic devices. In this paper, the three-dimensional (3D) electromagnetic (EM) simulation software MicroStripes7.5, which is based on the transmission line matrix (TLM) method, are employed to investigate the HEMP coupling effect on a wire located inside a cylindrical shielding cavity having one or few apertures. The EM models of the wire and the apertured shielding cavity are constructed, and the induced wire currents through the aperture of cavity are simulated. By comparing the simulation results of the wire with and without shield of the cavity, the shielding effectiveness (SE) is calculated. Further, the effects on induced wire in various cases are compared and analyzed, including single-aperture and multiple-aperture, different incident angles, polarization angles, and wire locations. Also, the cylindrical cavity is compared with the rectangular cavity.

Index Terms ─ Aperture, cylindrical cavity, EM simulation, HEMP, wire current.

I. INTRODUCTION

With the miniaturization of electronic and electrical equipments and systems, the electronic equipments become more sensitive and vulnerable to electromagnetic pulses (EMP). High altitude nuclear electromagnetic pulse (HEMP) is produced by nuclear explosion at high altitude, characterized by intense electric field strength, short duration, wideband frequency coverage and wide range coverage, which can damage electronic equipments of radar and communication systems, wires, crystal diodes, transistors, integrated circuits resistors, capacitors, filters, relays and other components. HEMP protection technologies and methods [1] have become one of the most important research fields in many applications.

Back door coupling through apertures is one of the main ways of HEMP attacks on the electronic devices. Some literatures have studied the methods of wire coupling effects of electromagnetic pulse. For example, the electromagnetic field energy flow on a thin wire is measured using Hallén integral equations [2]. Resonance of the wire is formulated using the theory of the linear antenna [3]. A 'diffuse-field reciprocity principle' has been applied to electromagnetic (EM) systems, enabling the currents induced in a wiring system to be computed in an efficient manner [4].

However, most of these researches focus on the coupling effects of unshielded wire. In practice, wires are often in enclosure by a shielding cavity for the electromagnetic pulse protection. Inevitably, if the shielding cavity has one or some apertures, the wire induced circuits will be produced through aperture coupling.

For aperture coupling, some methods have been proposed. An efficient hybrid method is developed for calculating EMP coupling to a device on a printed circuit board inside a cavity with an aperture [5]. The EM coupling through a thick aperture in multilayer planar circuits has been analyzed using extended spectral domain approach and finite difference time-domain

Submitted On: Oct. 30, 2011
Accepted On: April 25, 2012

(FDTD) method [6]. EMP coupling rules of different apertures is also researched and the rules of coupling energy are discussed in the condition of different polarization [7]. The fast prediction of the electromagnetic shielding performances of aperture loaded by resistive thin film coatings is investigated [8].

As for the shielding effectiveness (SE) of a cavity, the rectangular shielding cavity has been mostly studied so far, for example, the SE is evaluated for a rectangular enclosure with numerous apertures [9]. Based on the method of moments (MoM), the SE of rectangular enclosures with thin and thick Apertures has been analyzed [10]. The SE of rectangular metallic enclosures with apertures, metal plates, and conducting objects is calculated using fast MoM [11]. The SE of rectangular enclosures with apertures using transmission line matrix (TLM) method is analytically formulated [12]. However, a few are for the cylindrical shielding cavity.

In this paper, we will investigate the HEMP coupling effect on a wire which is located inside an apertured cylindrical shielding cavity using MicroStripes7.5, 3D EM simulation software. We will construct the EM models of the wire and the cylindrical shielding cavity with one or few apertures, and simulate to obtain the induced wire current through apertures of cavity. By comparing the simulation results of the wire with and without shield of the cavity, we calculate the shielding effectiveness. Further, we will compare and analyze the affects of induced wire currents under various conditions, including single-aperture and multiple-aperture, different incident angles, polarization angles and wire locations. Also, we compare our cylindrical cavity with traditional rectangular cavity.

II. EM SIMULATION SOFTWARE AND TLM METHOD

3D EM simulation software MicroStripes7.5 is used in this paper to analyze the HEMP coupling effect on a wire located in an apertured cylindrical shielding cavity. MicroStripes7.5 is based on the TLM method.

The TLM method is a time-domain, differential numerical technique for modeling electromagnetic and other field problems, especially for wideband incident wave coupling like HEMP. The details of the TLM theory can be found in [13]. Its computational efficiency, stability, and calculation accuracy have all been well proven. Also, TLM is unconditionally stable, the time step being determined by the mesh resolution. TLM has some advantages over frequency domain FDTD. Firstly, it can exactly calculate electric and magnetic fields on the same mesh, without the half cell offset characteristic of FDTD. In the TLM method, both space and time are in discrete form in order to implement Huygens' model on a digital computer, and the networks containing series and shunt nodes are adopted to simulate different situations of propagation. The currents of series-wound nodes are calculated in the scattering matrix [14]. The comparison between measurements and TLM method shows good agreement in analyzing a wire placed inside a rectangular cavity with an aperture [15].

MicroStripes7.5 software has been extensively used in vehicles, ships, aviation, and also employed in the evaluation of human absorption of electromagnetic fields, to solve the issues of antenna design, installation performance assessment, RF or microwave devices, radar cross section (RCS), electromagnetic compatibility (EMC), electromagnetic interference (EMI), electromagnetic pulse (EMP), and lightning strikes and other issues.

III. HEMP WAVEFORM

HEMP waveform standards promulgated by the standard of MIL-STL-461F [16] is adopted in this paper, the electric field description can be expressed as

$$E(t) = kE_p(e^{-\alpha t} - e^{-\beta t}) \qquad (1)$$

where $k = 1.3$, $E_p = 50kV/m$, $\alpha = 4\times10^7 s^{-1}$, $\beta = 6\times10^8 s^{-1}$.

We take an observation point in infinite space near the ground. HEMP incident wave in time domain and frequency domain can be simulated by MicroStripes7.5, as shown in Fig. 1.

It is shown from Fig. 1 that the HEMP energy mainly focuses on the frequency range of 200 ~ 300*MHz*, and the energy is small when the frequency is over 3GHz. Therefore, the following simulation and analysis of coupling currents focus on the frequency range of 0~3GHz.

In the following, except Section VI and VII, the HEMP incident angles of elevation is 10°, the

azimuth angles is 30°, and the polarization angle is 30°.

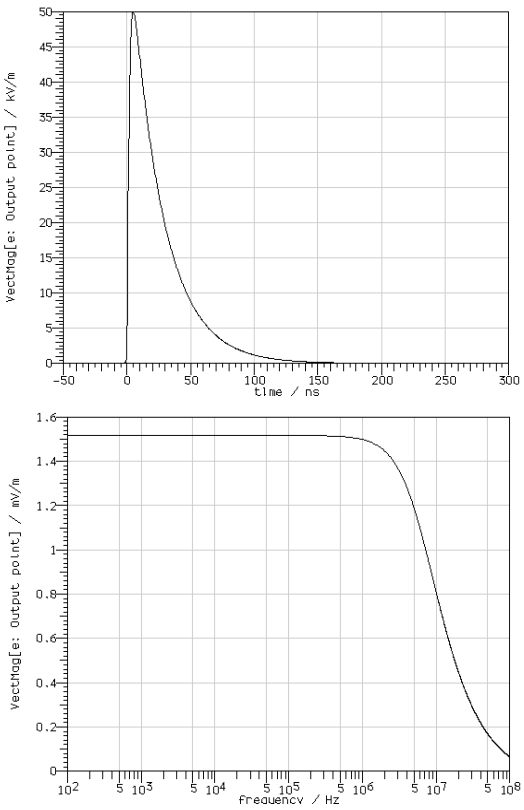

Fig. 1. HEMP incident wave in time domain and frequency domain described by MIL-STL-461F standard.

IV. SIMULATION MODELING AND ANALYSIS OF WIRE CIRCUIT IN A CYLINDRICAL SHIELDING CAVITY

A. Simulation Model

In this section, a wire and a cavity are modeled in the EM simulation. Their parameters are shown in Table 1.

Table 1: Parameters of the wire and cavity

	Radius	**Length**	**Wall thickness**	**Height above ground**
wire	0.25mm	13cm		11cm
cavity	5cm	20cm	0.5cm	6cm

The wire is assumed to be an ideal conductor line whose resistivity $\gamma \to 0$, being placed parallel to the ground, without a shield of a cavity. The model of an unshielded wire is built using the simulation software, shown in Fig. 2.

In Fig. 3, the wire is insulately located inside a cylindrical cavity with a single aperture. On the bottom of the cavity, there exists a rectangular aperture with the size of $0.5\text{cm} \times 3\text{cm}$. The conductivity of the cavity walls is 1×10^{7} s/m and the relative permeability is 200. Thus, we can consider the cavity walls as a nearly perfect conductor. The cavity is placed parallel to the ground, and is 6cm above to the ground.

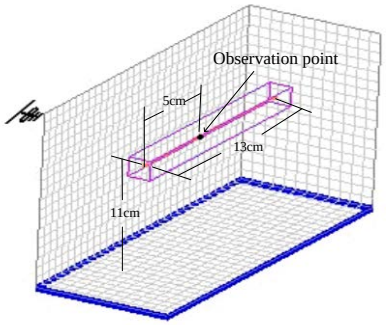

Fig. 2. The model of an unshielded wire.

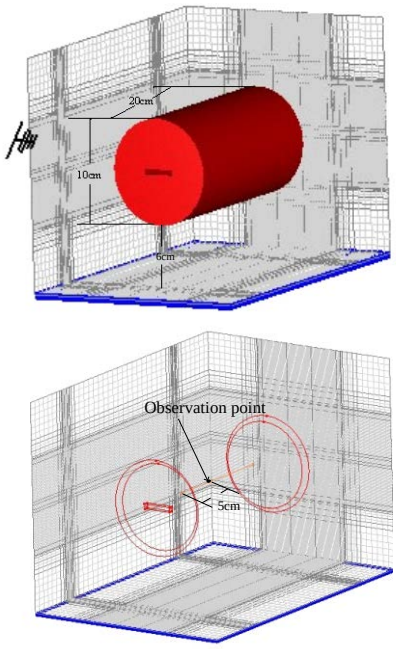

Fig. 3. The model of a wire inside a cylindrical cavity with a single aperture.

In the simulation, we put two observation points on the wire in Fig. 2 and Fig. 3, respectively. The observation point on the unshielded wire (without the cavity) is named as Ioutput1, and the observation point on the wire inside the cavity is named as Ioutput2. The two

observation points are all 5cm distances from the front terminal of the wire.

B. Results Analysis

The time-domain waveforms of Ioutput1 and Ioutput2 are shown in Fig. 4 and Fig. 5.

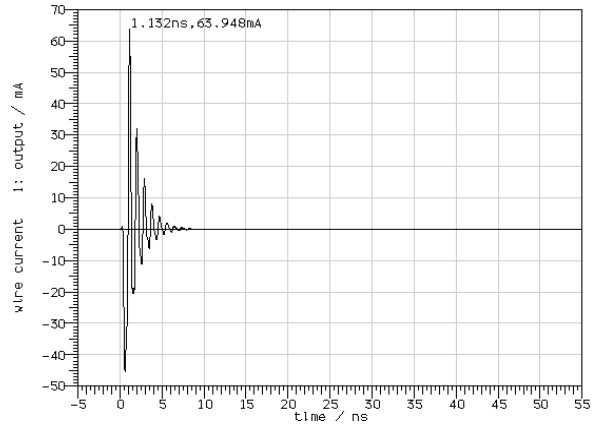

Fig. 4. Ioutput1's waveform of current in time domain.

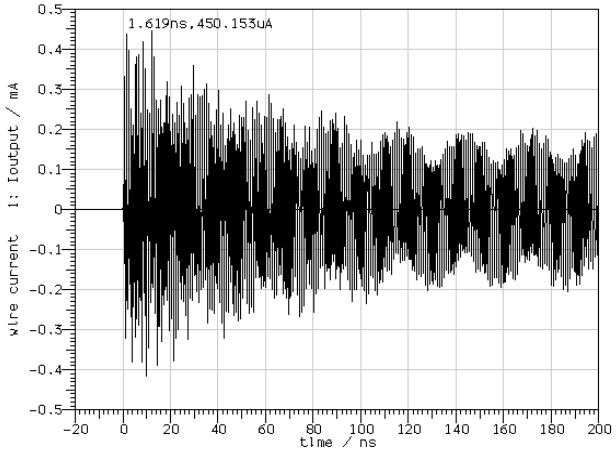

Fig. 5. Ioutput2's waveform of current in time domain.

Since the induced currents on the wire bounces back and forth due to reflection, waveform oscillation is formed, as shown in both Fig. 4 and Fig. 5. With the increase of time, the induced wire currents periodically oscillate and gradually attenuate. The maximum oscillation amplitude at Ioutput1 point is I_{o1} =63.948mA, occurring at the time of 1.132ns, and then it gradually decays to zero after 10ns.

The wire current inside the cavity is mainly high-frequency oscillating current due to the reflection of the cavity walls. Electromagnetic pulse energy is coupled into the shielding cavity and resonance is generated. Then high-frequency oscillatory current is induced in the wire. In the initial time, the amplitude of oscillation current is high, the maximum oscillation amplitude at Ioutput2 point is I_{o2} =450.153μA.

Therefore, compared with the wires with and without a shield of the cavity, the shielding effectiveness is $SE = 20\log\frac{I_{o1}}{I_{o2}} = 43dB$. That is, the induced wires current with a shield of the cavity is decreased by 43dB.

The frequency-domain waveforms of Ioutput1 and Ioutput2 are shown in Fig. 6 and Fig. 7 respectively. By analyzing the frequency spectrum, we can see that, within the frequency-range of 0~3GHz, the optimal coupling frequency is between 1.00GHz ~ 1.10GHz and 2.00GHz ~ 2.10GHz. Comparing the two figures, we can also see that, since the wire inside the cavity is shielded, the current components coupled into the wire are much smaller than the case of the wire without shielding cavity. From this, we know that the cavity with aperture plays a very good role of protection. In practice, specific evaluation of protective levels is based on the damage threshold of the electronic equipment inside the cavity.

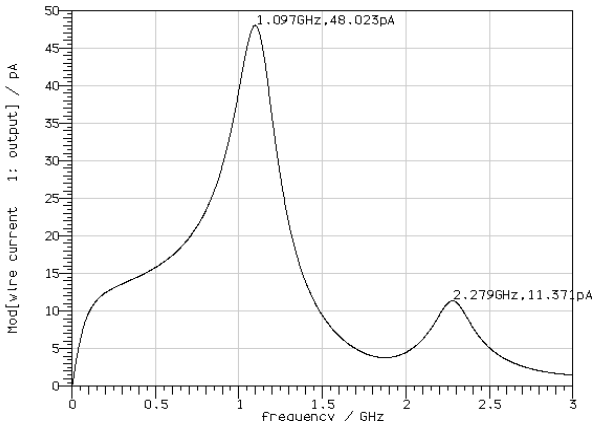

Fig. 6. Ioutput1's waveform of current in frequency-domain.

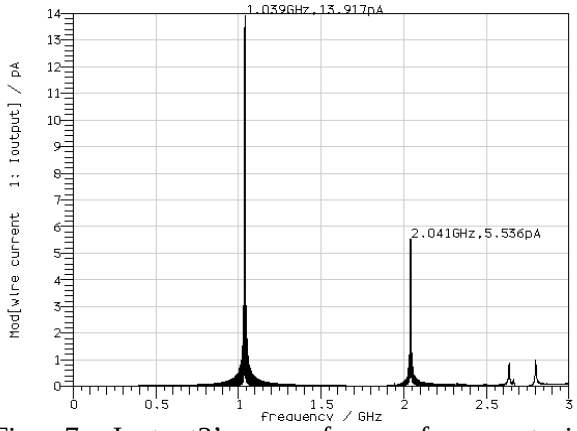

Fig. 7. Ioutput2's waveform of current in frequency-domain.

V. SIMULATION AND ANALYSIS OF THE IMPACT OF THE NUMBERS OF APERTURES

A. Simulation Model

In this section, we compare the impact of different numbers of apertures on the induced current based on two models. The two models are shown in Fig. 8 and Fig. 9, respectively.

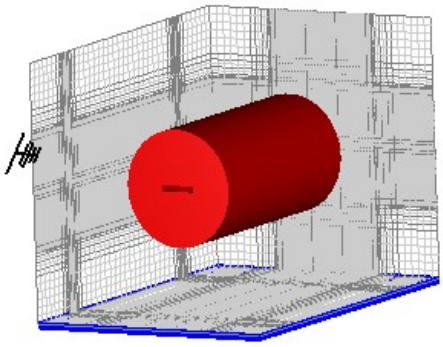

Fig. 8. Single aperture.

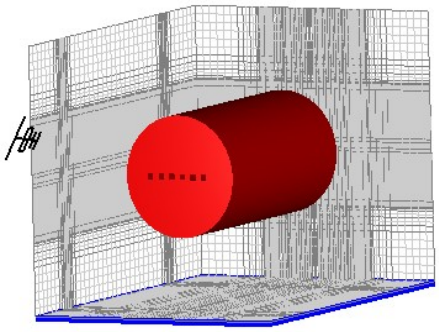

Fig. 9. Multiple apertures.

The material in both Fig. 8 and Fig. 9 is iron. The cavity parameters are the same as in Section IV. The single aperture model in Fig. 8 is a rectangular aperture with size of 0.5cm×3cm. The multiple aperture model in Fig. 9 are composed of six same squares with side length of 0.5cm, the total area of which is the same as in Fig. 8.

Inside the cavity, we insulately place a wire having the same parameters as in section IV. The observation points are 6cm distances from the front terminal of the wire.

B. Results Analysis

Figure 10 and Fig. 11 show the time-domain current waveforms of the wire located inside the cavities with single aperture and multiple apertures, respectively.

It is shown that the maximum coupling current peak of the wire inside the cavity with single-aperture is 449.889μA. However, the maximum value inside the cavity with multiple-aperture is 8.303μA, which is lower than that of the single-aperture cavity. Compared with single-aperture, the shielding effectiveness of multiple-aperture is increased by 34.7dB.

Therefore, by increasing the number of apertures the shielding effectiveness is much increased while keeping the total area the same. The reason can be analyzed similarly to the rectangular apertured cavity case in [12] using analytical formulation of shielding effectiveness modeling aperture as impedance.

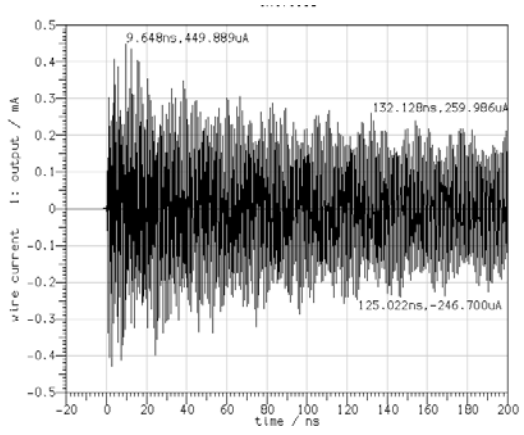

Fig. 10. Wire current waveform of single-aperture cavity.

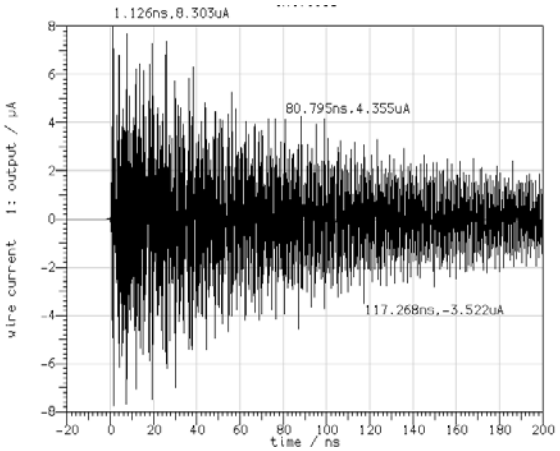

Fig. 11. Wire current waveform of multiple-aperture cavity.

VI. AFFECT OF THE INCIDENT ANGLE

In this section, we compare the affect of different HEMP incident angles. Figures 12 - Fig. 15 show the current waveform for different incident elevation angles, they are 0°, 10°, 60° and 90°.

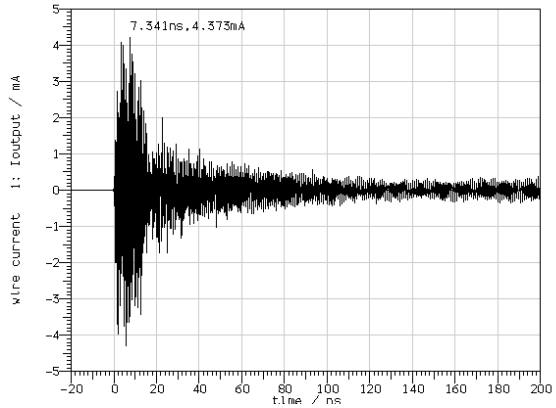

Fig. 12. Current waveform of 0° incident angle.

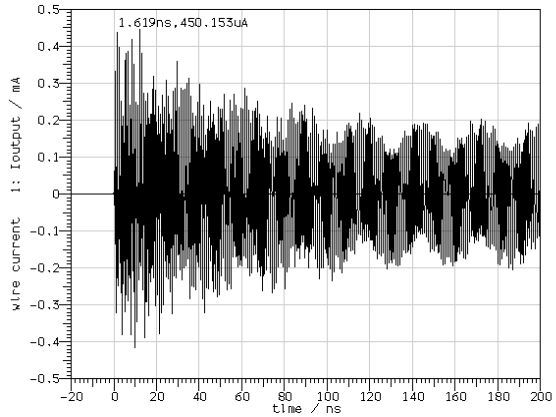

Fig. 13. Current waveform of 10° incident angle.

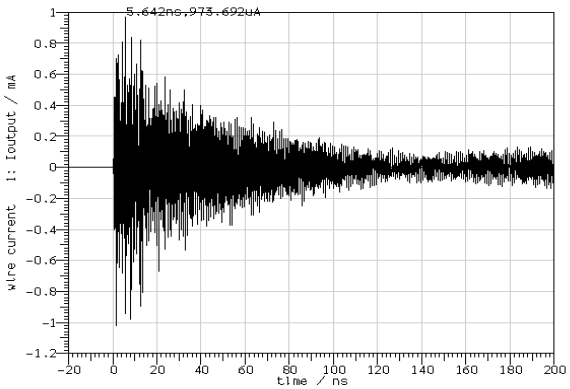

Fig. 14. Current waveform of 60° incident angle.

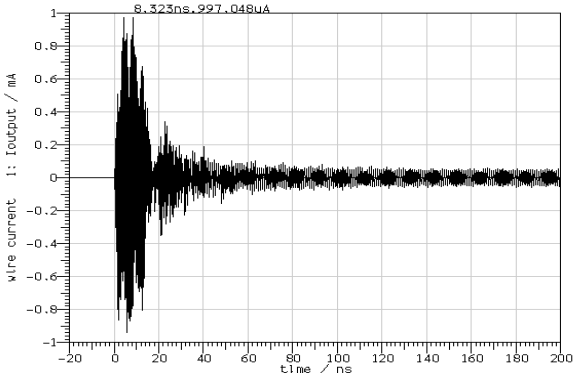

Fig. 15. Current waveform of 90° incident angle.

From Fig. 12 to Fig. 15, we know that on the condition of 0° incident angle, the current on the wire is the largest. The maximum amplitude is over 4mA. After the coupling of HEMP, the amplitude of the current oscillates in the range from 300μA to 450μA. For other incident angles, the maximum amplitude of the wire current during the coupling period is below 1mA, and changes very little with the change of the incident angle. The comparison of maximum current amplitude for different incident angles are listed in Table 2.

Table 2: The maximum current amplitude for different incident angles

Incident angle	0°	10°	60°	90°
Maximum current amplitude	4.373 mA	450.153 μA	973.692 μA	997.048 μA

VII. AFFECT OF THE POLARIZATION ANGLE

We further study the affect of different HEMP polarization angles while the incident angles are the same. Figure 16 - Fig. 19 show the current waveform in frequency-domain for different polarization angles, they are 0^o, 30^o, 60^o and 90^o.

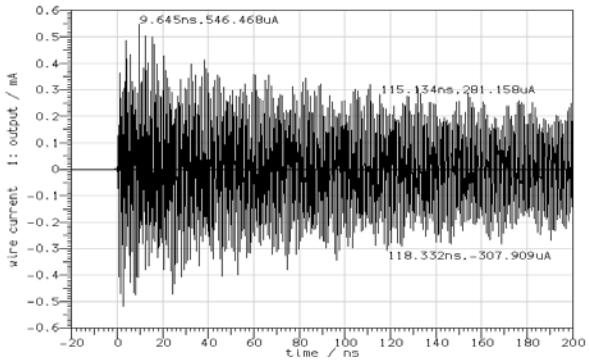

Fig.16. Current waveform of 0^o polarization angle.

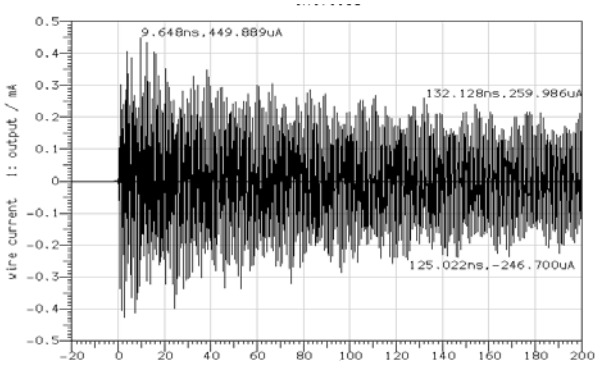

Fig.17.Current waveform of 30^o polarization angle.

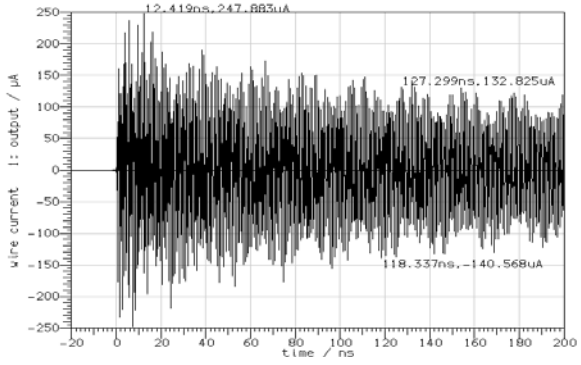

Fig.18.Current waveform of 60^o polarization angle.

From Fig. 16 to Fig. 19, we know that on the condition of 0° polarization angle, the current on the wire is the largest. Besides with the increase of the polarization angle, the amplitude of the current decreases. When the polarization angle is 90°, the current on wire decays the most fast. The comparing table of the currents' biggest amplitude in different cases is listed in Table 3.

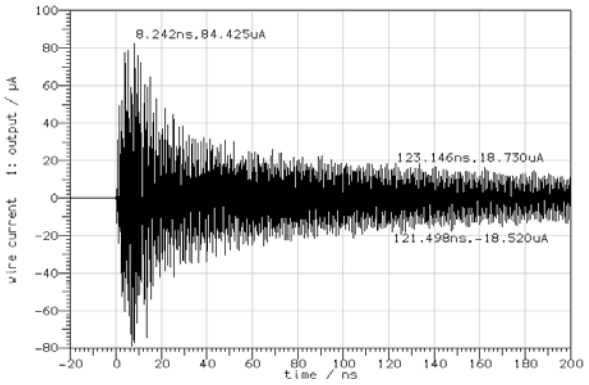

Fig.19. Current waveform of 90^o polarization angle.

Table 3: The maximum current amplitude for different polarization angles

Polarization angle	0°	30°	60°	90°
Maximum current amplitude	546.47 µA	449.9 µA	247.88 µA	84.425 µA

VIII. AFFECT OF THE LOCATION OF WIRE INSIDE THE CAVITY

In this section, two different locations of the wire inside the cavity are compared. The model and results analysis are shown as follows:

A. Simulation Model

The parameters of the cavity and the wire are the same as in Section IV. However, the wire is placed at two different locations in the cavity.

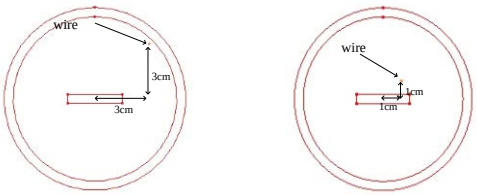

(a) The wire near to wall. (b) The wire near to aperture.

Fig. 20. Vertical vision of the wire location.

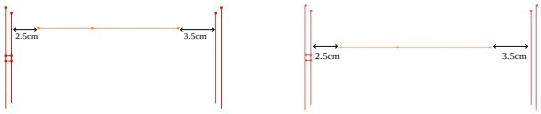

(a) The wire near to wall. (b) The wire near to aperture.

Fig. 21. Horizontal vision of the wire location.

Figure 20 and Fig. 21 show the vertical and horizontal visions of the wire location, respectively. The vertical and horizontal distances from the wire to the aperture and the cavity walls are shown in the figures.

B. Results Analysis

We put an observation point in the wire to observe the wire current, shown in Figure 21. The observation point in Figure 21(a) is named as I(1), and in Figure 21(b) is named as I(2).

Figure 22 shows the time-domain waveform on the wire, and Fig. 23 shows the frequency-domain waveform.

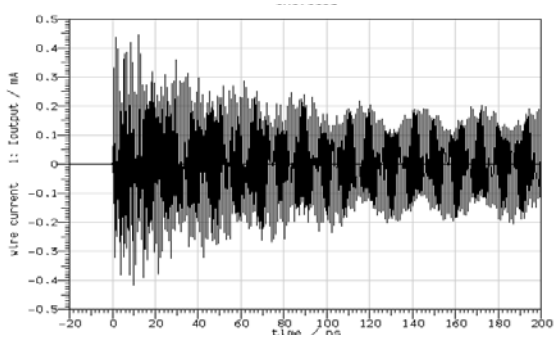

(a) The time-domain waveform of I(1)

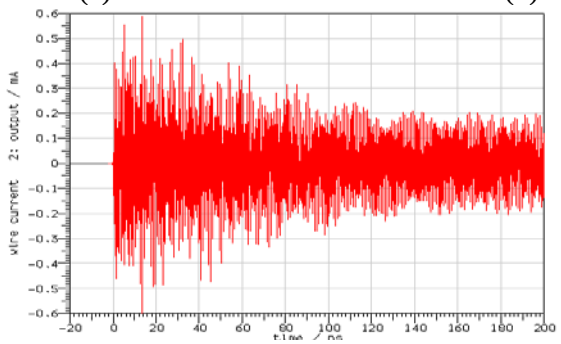

(b) The time-domain waveform of I(2)

Fig. 22. The current waveform in time domain.

By comparing the two conditions, we know that the optimal coupling frequency is between the 1.0 GHz - 1.10GHz and 2.0GHz - 2.2GHz, and the value of the amplitude changes with the changing of the wire's location. In the time-domain, the current maximum amplitude of I(1) is about 0.44mA, and current maximum amplitude of I(2) is about 0.59mA. The coupling affect of the aperture is stronger than that of the cavity wall.

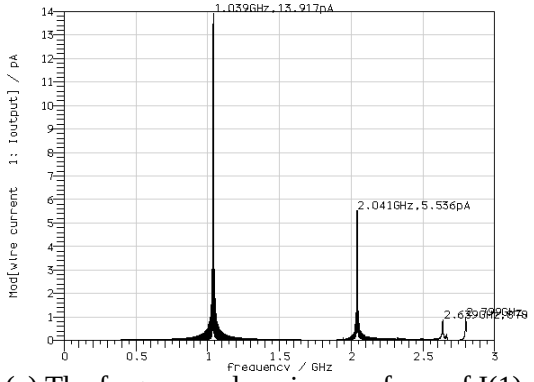

(a) The frequency-domain waveform of I(1)

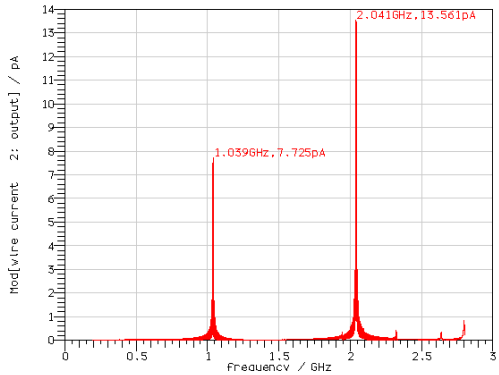

(b) The frequency-domain waveform of I(2).

Fig. 23. Current waveform in frequency-domain.

IX. COMPARISION BETWEEN CYLINDRICAL CAVITY AND RECTANGULAR CAVITY

A. Simulation Model

The size of the cylindrical cavity is the same as in section IV. The rectangular cavity has the parameters as follows: Its side length of the square bottom is 10cm, its length is 20cm, and its wall thickness is 0.5cm. The size of the aperture is also 0.5cm×3cm. Figure 24 shows the model of a wire inside a rectangular cavity with a single aperture. The wire is placed at the same location relative to the aperture as in the cylindrical cavity.

B. Results Analysis

For different shapes of cavity, the time-domain waveform is shown in Fig. 25 and Fig. 26. The amplitude value of the optimal coupling frequency is shown in Fig. 27 and Fig. 28.

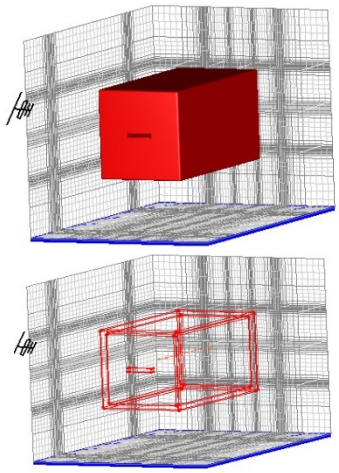

Fig. 24. The model of a wire inside a rectangular cavity with a single aperture.

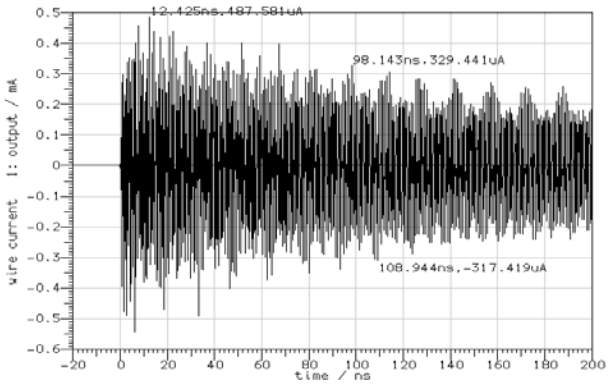

Fig. 25. The waveform of wire current for rectangular cavity.

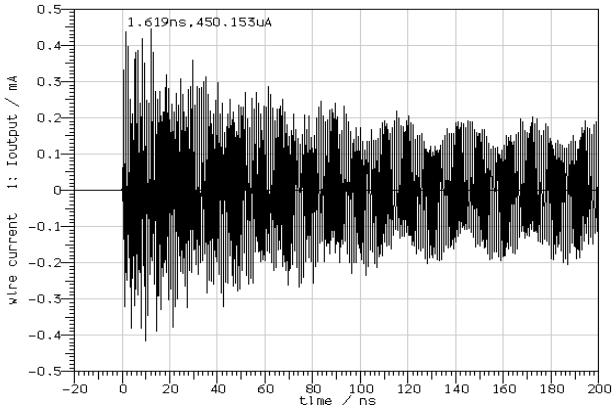

Fig. 26. The waveform of wire current for cylindrical cavity.

For the rectangular cavity, the maximum current amplitude is about 487.581μA, the amplitude of high-frequency oscillating current is about 300μA after the coupling of HEMP, the two optimal coupling frequencies are 1.072GHz and 2.075GHz, and the their corresponding amplitudes are respectively 12.446pA and 2.695pA. While for the cylindrical cavity, the maximum current amplitude is about 449.889μA, the amplitude of high-frequency oscillating current is about 250μA after the coupling of HEMP, the two optimal coupling frequencies of the cylindrical cavity is 1.054GHz and 2.064GHz, and their corresponding amplitudes are respectively 10.7pA and 3.919pA.

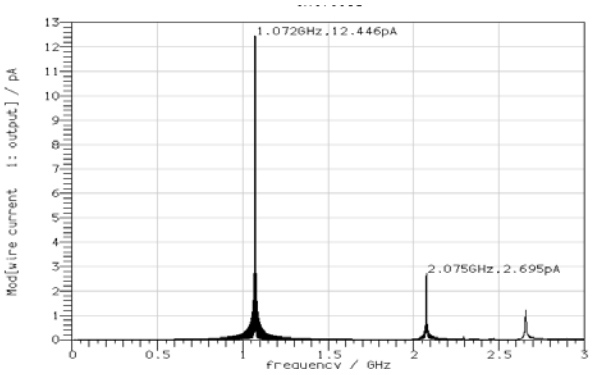

Fig. 27. The current amplitue of the optimal coupling frequency in rectangular cavity.

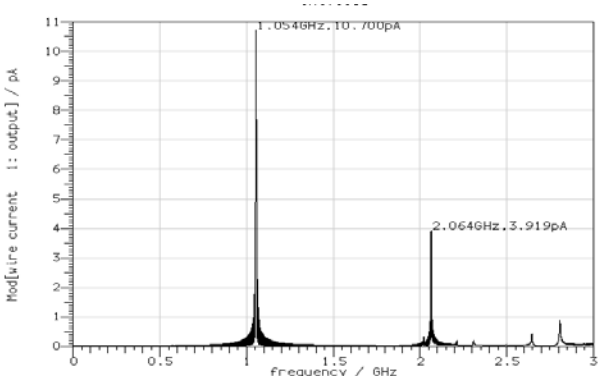

Fig. 28. The current amplitue of the optimal coupling frequency in cylindrical cavity.

X. CONCLUSION

In this paper, we exploit the EM simulation software MicroStripes 7.5 to simulate the environment of HEMP, modeling and analyzing the effect of HEMP coupling on the wire which is inside a shielding cylindrical cavity with apertures. Under the model of this experiment, the induced currents on the wire shielded by an apertured cavity are decreased about 43dB compared with on the wire without cavity. Aperture characteristic is the main factor which determines the strength of HEMP coupling to the cavity. When the total area

of the aperture is the same, the coupling coefficient of multiple-apertured cavity is much smaller than that of single-apertured cavity. Compared with single-aperture, the shielding effectiveness of multiple-aperture is increased by 34.7dB. When the HEMP incident elevation angle is 0° and the polarization angle is 0°, the induced current on the wire is larger than other angle cases. While the wire is near to the aperture, its induced current is larger than the case when the wire is near to the wall. Also, since the rectangular cavity and the cylindrical cavity of cavities have similar volume and size, the optimal coupling frequency and the amplitude of the high frequency components for the two shapes is close, the latter is a little bit smaller than the former in our simulation.

ACKNOWLEDGMENT

The authors would like to thank the reviewers for their useful comments and suggestions.

REFERENCES

[1] X. J. Zhang, J. Yang, Q. Y. Yuan, Z. X. Wang, X. J. Li, "Research on the Suppressing Behaviour of EMP Protection Device," *Cross Strait Quad-Regional Radio Science and Wireless Technology Conf.*, vol. 1, pp. 318-321, 2011.

[2] D. Poljak, V. Doriæ, V. Roje, "Transient Analysis of Buried Cables," *Proc. IEEE International Symposium on Antennas and Propagation*, Washington, USA: IEEE Press, vol. 1B, pp. 46-49, 2005.

[3] J. M. Myers, S. S. Sandler, T. T. Wu, "Electromagnetic Resonances of a Straight Wire," *IEEE Trans. Antennas Propagat*., vol. 59, no. 1, pp. 129-134, 2011.

[4] R. S. Langley, "A Reciprocity Approach for Computing the Response of Wiring Systems to Diffuse Electromagnetic Fields," *IEEE Trans. Electromagnetic Compatbility*, vol. 52, no. 4, pp. 1041-1055, 2010.

[5] C. Lertsirimit, D. R. Jackson, and R. Wilton, "An Efficient Hybrid Method for Calculating the EMC Coupling to a Device on a Printed Circuit Board inside a Cavity by a Wire Penetrating an Aperture," *Electromagnetics*, vol. 25, pp. 637-654, 2005.

[6] A. M. Tran, B. Houshmand, T. Itoh, "Analysis of Electromagnetic Coupling Through a Thick Aperture in Multilayer Planar Circuits Using the Extended Spectral Domain Approach and Finite Difference Time-Domain Method," *Antennas and Propagation*,vol.43, pp.921-926, 1995.

[7] A. Gademann, I. V. Shvets, C. Durkan, "Study of Polarization-dependent Energy Coupling between Near-field Optical Probe and Mesoscopic Metal Structure," *Journal of Applied Physics*, vol. 95, pp. 3988-3993, 2004.

[8] M. D'Amore, V. De. Santis, M. Feliziani, "Fast Prediction of the Electromagnetic Shielding of Small Apertures Coated by Conductive Thin Film," *2010 Asia-Pacific International Symposium on Electromagnetic Compatibility (APEMC)*, pp. 524-527, 2010.

[9] P. Dehkhoda, A. Tavakoli, R. Moini, "An Efficient and Reliable Shielding Effectiveness Evaluation of a Rectangular Enclosure with Numerous Apertures," *IEEE Trans. Electromagnetic Compatibility*, vol. 50, no. 1, pp. 208-212, 2008.

[10] R. Araneo and G. Lovat, "An Efficient MoM Formulation for the Evaluation of the Shielding Effectiveness of Rectangular Enclosures with Thin and Thick Apertures," *IEEE Trans. Electromagnetic Compatibility*, vol. 50, pp. 294-304, 2008.

[11]R. Araneo and G. Lovat, "Fast MoM Analysis of the Shielding Effectiveness of Rectangular Enclosures with Apertures, Metal Plates, and Conducting Objects," *IEEE Trans. Electromagnetic Compatibility*, vol. 51, pp. 274-283, 2009.

[12]M. P. Robinson,T. M. Benson, C. Christopoulos, etc., "Analytical Formulation for the Shielding Effectiveness of Enclosures with Apertures," *IEEE Trans. Electromagnetic Compatibility*, vol. 40, pp. 240-248, Aug. 1998.

[13] WJR Hoefer, "The Transmission Line Matrix Method—Theory and Applications," *IEEE Trans, Microwave Theory and Tech.* vol. MTT-43, no. 9, pp. 882-893, Oct. 1985.

[14]A. F. Yagli, J. K. Lee, and E. Arvas, "Monochromatic Scattering from Three-dimensional Gyrotropic Bodies Using the TLM Method," *Applied Computational Electromagnetic Society (ACES) Journal*, vol. 22, no. 1, pp. 155-163, 2007.

[15]A. P. Duffy, T. M. Benson, and C. Christopoulos, "Propagation Along a Wire Placed Inside a Cavity with an Aperture: A Comparison of Measurements and Transmission-Line Modeling (TLM)," *IEEE Trans. Electromagnetic Compatibility*, vol. 36, pp. 144-146, 1994.

[16]Requirements for the Control of Electromagnetic Interference Characteristics of Subsystems and Equipment [S], MIL-STD-461F, Re 10, December 2007.

Shu-Ting Song received the B.S. degree in Communication Engineering from Jilin University, China, in 2010. She is currently a graduate student at College of Communication Engineering, Jilin University, China. Her current research interest is EM simulation in computational electromagnetics.

Hong Jiang received the B.S. degree from Tianjin University, China, in 1989, the M.S. degree in Communication and Electronic System from Jilin University of Technology, China, in 1996, and the Ph.D. degree in Communication and Information System from Jilin University, China, in 2005. From May 2010 to May 2011, she had worked as a visiting research fellow at McMaster University, Canada. Currently, she is an associate professor at the College of Communication Engineering, Jilin University, China. She is a senior member of the Chinese Institute of Electronics (CIE). Her research fields focus on electromagnetic protection, signal processing for wireless communication. She has published over 40 papers.

Yu-Lan Huang is an associate professor at the College of Communication Engineering, Jilin University, China. Her current research fields involve simulation of wireless communication networks and microwave technology.